

Edge Aware Learning for 3D Point Cloud

Lei Li

arXiv:2309.13472v2 [cs.CV] 25 Oct 2023

Abstract This paper proposes an innovative approach to **Hierarchical Edge Aware 3D Point Cloud Learning (HEA-Net)** that seeks to address the challenges of noise in point cloud data, and improve object recognition and segmentation by focusing on edge features. In this study, we present an innovative edge-aware learning methodology, specifically designed to enhance point cloud classification and segmentation. Drawing inspiration from the human visual system, the concept of edge-awareness has been incorporated into this methodology, contributing to improved object recognition while simultaneously reducing computational time. Our research has led to the development of an advanced 3D point cloud learning framework that effectively manages object classification and segmentation tasks. A unique fusion of local and global network learning paradigms has been employed, enriched by edge-focused local and global embeddings, thereby significantly augmenting the model’s interpretative prowess. Further, we have applied a hierarchical transformer architecture to boost point cloud processing efficiency, thus providing nuanced insights into structural understanding. Our approach demonstrates significant promise in managing noisy point cloud data and highlights the potential of edge-aware strategies in 3D point cloud learning. The proposed approach is shown to outperform existing techniques in object classification and segmentation tasks, as demonstrated by experiments on ModelNet40 and ShapeNet datasets.

Keywords 3D Point Cloud · Edge Learning · Classification · Segmentation

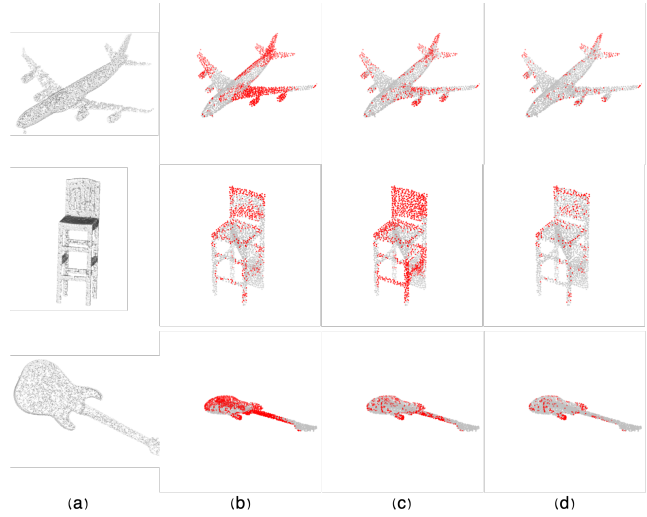


Fig. 1 Our study applies edge-aware sampling to point cloud data at varying complexities—1024, 512, and 256 points—demonstrating consistent preservation of critical object geometry and topology information, irrespective of the reduction in point complexity. (a) Original point cloud; (b, c, d) edge-aware sampling.

1 introduction

Point clouds, a versatile data representation format, are central to numerous fields such as autonomous driving, augmented reality, and robotics. With the rise of advanced 3D sensing technologies, the acquisition of 3D data has become notably accessible, leading to the creation of an array of online data repositories, including ModelNet[1], ShapeNet[2], and ScanNet[3]. Amidst the variety of 3D shape representations, including voxel, mesh, and multi-view images, point clouds stand out as the preliminary data captured by LiDAR or depth cameras, like Kinect. The robust utility of point cloud data, underpinned by the critical task of representative

point sampling, is evidenced in its broad applications, from scene reconstruction and autonomous driving navigation to virtual reality. As such, the development of efficient point cloud learning algorithms remains a significant focus in contemporary scientific and technological research.

Within the realm of 3D data processing, point cloud sampling methodologies, such as random sampling (RS), grid sampling, uniform sampling, farthest point sampling (FPS)[4], and geometric sampling, are foundational. RS, while boasting efficiency, tends to overlook sparser regions, and FPS, despite its wide coverage, is hindered by latency issues during parallel operations. The application of grid sampling, through its use of regular grids, lacks the ability to accurately control the number of sampled points. Uniform sampling, renowned for its robust nature, evenly distributes the points chosen across the cloud. Geometric sampling strategies that focus on local geometric properties, like shape curvature, along with techniques like Inverse Density Importance Sampling (IDIS) that favor points with lower cumulative distances to neighbors, call for high-density point clouds for maximum efficacy.

Yet, in spite of the advancements brought about by these traditional methodologies, the preservation of geometric information during the sampling process, particularly for complex objects with nuanced topology structures and irregular surface morphology, remains a daunting challenge. This obstacle has led to the emergence of cutting-edge learn-to-sample methods that concurrently optimize both the sampling process and specific downstream tasks. Such innovations have made substantial contributions to domains such as point cloud classification and reconstruction. Nonetheless, the challenge of maintaining geometric integrity within complex objects is still a largely unexplored area in academic research. In light of the vast diversity of object topological structures, defining a consistent category-agnostic edge at the semantic level poses a significant non-trivial challenge. Current datasets typically encompass only singular or a limited range of known object categories. Additionally, topological methods, which are ordinarily category-agnostic, concentrate predominantly on the geometric and topological attributes of the shape, such as its connectivity, topology, length, direction, and width.

With the advancement of deep learning techniques, several neural network-based sampling methods, such as S-Net [5], SampleNet[6], and DA-Net[7], have emerged. These approaches leverage multi-layer perceptrons (MLPs) to produce resampled point cloud sets of prescribed sizes, with MOPS-Net offering an innovation of generating a sampling transformation ma-

trix. Despite their novelty, these methods lean toward a generative approach, bypassing direct point selection. Meanwhile, research has grown around creating neural network-based local feature aggregation operators for point clouds. However, these techniques, while reducing point numbers during latent feature learning, don't strictly qualify as sampling methods as they lack real spatial points during processing. Furthermore, the complex task of skeleton extraction adds another layer of complexity due to the inherent diversity of object topological structures and sensitivity to surface noise.

By leveraging deep neural networks to learn object edges, a prior probability for sampling each point, mindful of edge-awareness, can be established. To adapt edge-aware sampling for subsequent tasks, we synergistically optimize the posterior sampling probability for each point. This process is achieved in an end-to-end manner, utilizing the transformative capabilities of transformer neural network architectures.

Actually, the performance of machine learning models is often constrained by the presence of noisy points within the cloud, thereby calling for the evolution of techniques capable of robustly managing such data. The concept of edge-awareness is inspired by the human visual system that profoundly relies on edge or part information for object recognition. The integration of such edge-aware strategies into point cloud learning can augment recognition capacities and concurrently decrease computational time. In this study, we introduce an edge-aware learning methodology that significantly bolsters point cloud classification and segmentation, contributing in three keypoints:

- We propose an innovative, edge-aware 3D point cloud learning framework handling object classification and segmentation.
- The fusion of local and global network learning paradigms, further supplemented by corresponding edge-focused local and global embeddings that enrich the model's interpretive abilities.
- The application of a hierarchical, transformer architecture that enhances point cloud processing efficiency, offering sophisticated insight into structural understanding.

2 Related Work

Point Cloud Sampling. The paramountcy of point cloud sampling in processing high-resolution dense point clouds is undeniable, and this recognition has precipitated the development of an array of innovative methods. Some techniques, for instance, harness K-means clustering to highlight representative points,

concurrently removing redundancy. Others combine the power of clustering with a coarse-to-fine methodology to enhance point cloud processing efficiency. Intrinsic point cloud algorithms, providing a guarantee of density, further contribute to this field, facilitating uniform and feature-sensitive resampling. However, these strategies tend to concentrate on subset identification based on geometric or topological criteria, often overlooking the downstream task implications during sampling.

In recent years, the advent of learn-to-sample approaches has heralded a new era in this domain. These methodologies introduce learning-based [6, 8, 9, 10], task-oriented sampling strategies [11, 12] explicitly designed to cater to downstream tasks like point cloud classification, retrieval, and reconstruction. Some approaches incorporate a learnable sampling and joint-training strategy, mitigating overfitting risks for specific tasks. Others innovatively embed a critical point layer, transferring points with the most functional features to subsequent layers to enable adaptive fusion sampling. Moreover, these learning-based techniques often outperform the traditional non-learning-based sampling methods, such as the well-known FPS, emphasizing the continued evolution in this field.

Point Cloud Representation Learning. Deep learning methodologies have become integral to point cloud analysis, exhibiting pervasive influence across a spectrum of areas such as point cloud classification/segmentation [2, 6, 13, 14, 15, 16, 17, 18], object detection/tracking [19], point cloud autoencoders [11], generation, completion, regression [20, 21, 22], and registration. The inherent complexity associated with the unstructured nature of point clouds, where the points are not positioned on a regular grid and exhibit varying degrees of mutual independence and inconsistent distances to neighboring points, presents significant challenges to the application of deep learning techniques.

An innovative breakthrough in this regard has been the advent of PointNet [13], a trailblazing strategy that applied deep neural networks to point sets for the first time. This framework converted the input into high dimensional space on a point-wise basis and subsequently employed a symmetric function to aggregate all point features, achieving a permutation-invariant global feature representation. This method led to the widespread adoption of the Multi-Layer Perceptron (MLP) block within many point cloud networks to learn point-wise representations. Then, PointNet++ [14], refined this approach further by considering local information, thereby enhancing the representational capacity and efficiency of the network. The Dynamic Graph CNN (DGCNN) [17], proposed EdgeConv blocks to dynam-

ically update the neighborhood information based on dynamic graphs, leading to superior point cloud analysis performance. In a similar vein, KPConv [11] proposed point-wise convolution operators for point cloud feature learning.

Alongside these convolution-based approaches, attention-based methods have also gained traction. For instance, Point Cloud Transformer (PCT) [19, 23] pioneered the use of self-attention layers in place of encoder layers within the PointNet framework. Another notable attention-based network, the Lightn [24], uses offset attention blocks to capture contextual information with light-weight transformer. These recent advancements demonstrate the potential of attention-based methodologies in capturing both local and long-range contextual information in the point cloud domain.

Edge Learning. The incorporation of edge or skeleton learning has emerged as a fundamental aspect for capturing crucial properties such as geometry, topology [25], and symmetry [12, 26, 27, 28] in objects, providing a concise and intuitive representation. This representation has demonstrated its efficacy across diverse computer vision tasks, encompassing shape recognition, reconstruction, segmentation, and point cloud completion. For instance, deep learning techniques have been proposed to leverage edge-awareness in generating mesh reconstructions of object surfaces from single RGB images. In the realm of image processing, the detection of edges typically relies on well-established techniques such as the Canny edge detector, which involves a multi-stage algorithm encompassing Gaussian filtering, intensity gradient computation, gradient magnitude thresholding, double thresholding, and edge suppression. These techniques enable the identification and extraction of salient edges while effectively suppressing weaker and disconnected ones, thereby enhancing the edge-aware analysis and interpretation capabilities.

3 Methods

We introduce our **Hierarchical Edge Aware 3D Point Cloud Learning (HEA-Net)** framework, which incorporates global and local learning for capturing edge information effectively. The framework uses deep tier learning, which processes the point cloud at different tiers to learn hierarchical features, similar to the workings of a human visual system. A detailed discussion of the architecture, layers, and algorithms involved is provided.

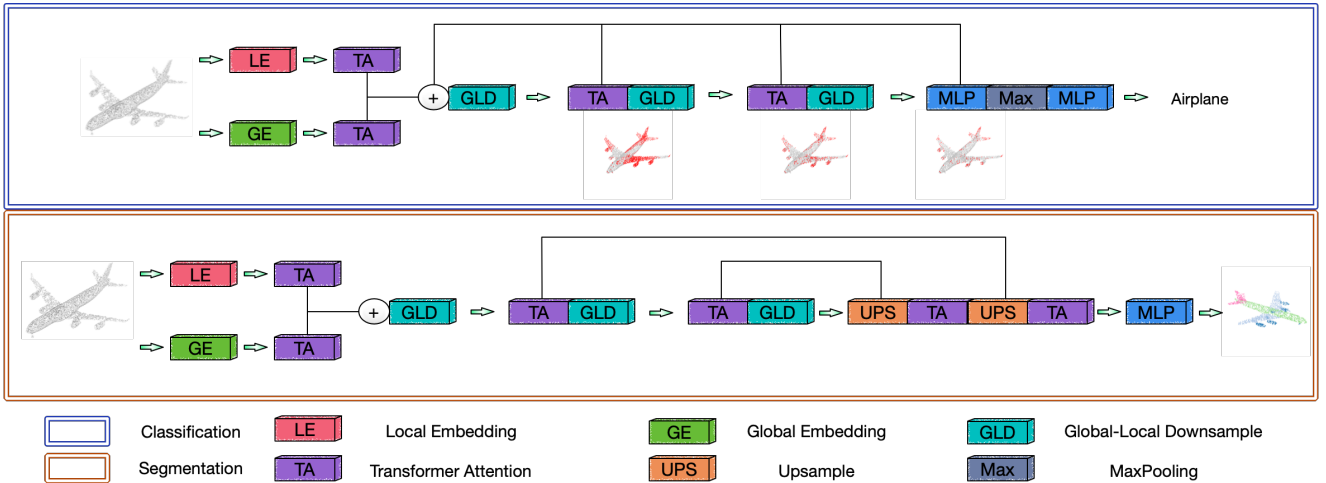


Fig. 2 The Hierarchical Edge-Aware network (HEA-Net) architectures employ distinctive strategies for classification(above) and segmentation(below) tasks. For classification and segmentation, the architecture combines local and global embeddings to effectively learn edge features, followed by an innovative global-local downsampling process that reduces a point cloud’s complexity from N to M points. On the other hand, in the context of segmentation, an upsample layer is introduced to augment the point cloud’s complexity back from M to N points. Integral to the HEA network’s process is the use of transformer-based attention mechanisms which enable the architecture to focus on and learn critical sampling features.

3.1 Overview of Framework.

The figure 2 illustrates our proposed Hierarchical Edge-Aware Network (HEA-net), which is specifically designed to adeptly execute classification and segmentation tasks for point clouds. A key aspect to note is the consistent application of the downsampling process across both classification and segmentation tasks. Subsequent to the application of local and global embeddings, the resultant data is fused and then fed into a multi-level network, specifically the Global-Local Downsampling (GLD) module. Evidently, from the classification tasks, it is apparent that the multi-layer downsampling accentuates the contours and edges of the object (in this case, an airplane). This approach efficiently discards superfluous information, thereby enhancing the pipeline’s accuracy and speed, making the HEA-net an effective tool for processing and interpreting point cloud data.

Within the scope of the classification task, the point cloud’s maximal feature is ultimately classified via the max pooling module. Conversely, in the context of segmentation tasks, a sequence of downsampling followed by upsampling is executed prior to conducting the segmentation. It is worth noting that two skip connections have been incorporated within the entire network structure. These skip connections significantly enhance the network’s ability to learn hierarchical features. Subsequently, we will delve into a detailed exposition of the embedding, downsampling, and transformer attention modules, further elucidating their pivotal roles in

the overall architecture of the Hierarchical Edge-Aware Network.

3.2 Embedding learning.

Algorithm 1 succinctly delineates the process of obtaining local and global points through the CenterNeighbor and CenterDiff operations, where neighbor selection is conducted using the K-Nearest Neighbor (KNN) method. The number of neighbor points to be selected is pre-determined by assigning a value to K . Notably, the choice of K can influence the overall performance and speed of the process. Theoretically, there exists a critical value for K beyond which performance improvements plateau [29].

Upon the selection of neighbor points, local features are sampled using these points, while global features are extracted by randomly selecting distant points that are not included within the neighborhood. It’s crucial to note that this extraction process differs from the Farthest Point Sampling (FPS) method. Following the embedding of these points, multi-level feature learning is then applied, thus facilitating a more nuanced understanding of the data at various scales.

3.3 Global and Local Learning for the Edge.

Algorithm 2 provides a detailed overview of the Hierarchical Global-Local Downsample algorithm. Q , K , and V parameters are derived utilizing a transformer-based approach, followed by a direct implementation of

Algorithm 1 CenterNeighbor and CenterDiff Procedures

```

procedure CENTERNEIGHBOR( $pcd \in \mathbb{R}^{B \times C \times N}$ ,  $K$ )
   $neighbors \leftarrow$  SELECTNEIGHBORS( $pcd$ ,  $K$ , "neighbor")
   $pcd_{repeated} \leftarrow$  Repeat  $pcd$   $K$  times across a new dimension
   $output \leftarrow$  Concatenate  $pcd_{repeated}$  and  $neighbors$  along channel dimension return  $output$ 
end procedure
procedure CENTERDIFF( $pcd \in \mathbb{R}^{B \times C \times N}$ ,  $K$ )
   $diff \leftarrow$  SELECTNEIGHBORS( $pcd$ ,  $K$ , "diff")
   $pcd_{repeated} \leftarrow$  Repeat  $pcd$   $K$  times across a new dimension
   $output \leftarrow$  Concatenate  $pcd_{repeated}$  and  $diff$  along channel dimension return  $output$ 
end procedure

```

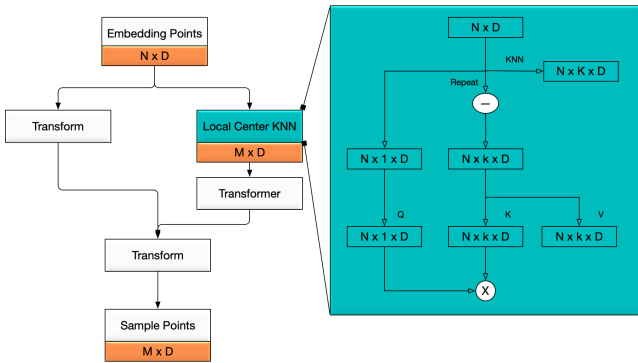


Fig. 3 Hierarchical downsampling combined with global feature and local feature for the edge.

global correspondence learning. Conversely, the Local-Downsample process acquires neighbor points through the K-Nearest Neighbor (KNN) method, subsequently employing attention mechanisms to discern the relationships between the neighbor points and the feature points.

As depicted in the corresponding Figure 3, point cloud information from the multi-scale fused embedding is integrated via local and global attention operations. Post-fusion, the dimension of the output point cloud stands at $N * D$. This output is then subjected to a downsampling procedure, yielding $M * D$ data. So, combined with Embedding layers, we can use hierarchical global and local feature to downsampling the point cloud. The global and local correlation maps, denoted as M^g and M^l , are combined into a single $N \times 2N$ correlation matrix M :

$$M = \begin{bmatrix} -m_1^{gT} & - & m_1^{lT} & - \\ -m_2^{gT} & - & m_2^{lT} & - \\ \vdots & & \vdots & \\ -m_N^{gT} & - & m_N^{lT} & - \end{bmatrix} \quad (1)$$

Algorithm 2 Hierarchical Global-Local DownSample Procedures

```

procedure GLOBALDOWNSAMPLE( $x \in \mathbb{R}^{B \times C \times N}$ )
  Compute  $q, k, v \leftarrow$  Transformer operations on  $x$ 
  Compute energy  $E \leftarrow q@k$ 
  Compute attention  $A \leftarrow \text{softmax}(E)$ 
  Compute selection  $S \leftarrow$  sum  $A$  across last dimension
  Select top  $M$  indices  $idx$  from  $S$ 
  Select scores by gathering  $A$  across index  $idx$ 
  Compute output  $out \leftarrow$  scores @  $v$ 
end procedure

procedure LOCALDOWNSAMPLE( $x \in \mathbb{R}^{B \times C \times N}$ )
  Compute neighbors of  $x$  and  $q, k, v \leftarrow$  Transformer operations
  Compute energy  $E \leftarrow q@k$ 
  Compute attention  $A \leftarrow \text{softmax}(E)$ 
  Compute selection  $S \leftarrow$  std. deviation of  $A$ 
  Select top  $M$  indices  $idx$  from  $S$ 
  Select scores by gathering  $A$  across index  $idx$ 
  Compute output  $out \leftarrow$  scores @  $v$ 
end procedure

procedure GLOBALLOCALDOWNSAMPLE( $x \in \mathbb{R}^{B \times C \times N}$ )
  Compute  $global_{out} \leftarrow$  GLOBALDOWNSAMPLE( $x$ )
  Compute  $local_{out} \leftarrow$  LOCALDOWNSAMPLE( $x$ )
  Compute output  $out \leftarrow global_{out} + local_{out}$ 
end procedure

```

In the combined correlation matrix M , let m_{ij}^g and m_{ij}^l represent the values at the i -th row and j -th column in the M^g and M^l partitions of M respectively. If point i is an edge point, its corresponding m_i^g will have a larger standard deviation, indicating that point j is also likely to be an edge point due to the large m_{ij} .

Instead of computing row-wise standard deviations as previously done, we propose to compute column-wise sums. Let $u_j = \sum_i m_{ij}$, where m_{ij} are the elements of M^g . We sample points that have a higher value of u_j . The underlying rationale is that a point which contributes more to the self-attention correlation map as a representative feature.

To create M^l , we use the (latent) features of the center point p_i as the query input and the feature difference between the neighbor point and the center point ($p_j - p_i$) as the key input. As per the original Transformer model, we employ the square root of the feature dimension count (\sqrt{d}) as a scaling factor. The final normalized correlation map m_i^l is thus given as follows:

As demonstrated in Figure 4, the feature information of the object post three hierarchical downsamplings and the final point cloud backcalculation is distinctly evident. Upon completion of the final sampling process, the M -dimensional information manifests as an effective representation of the object's information, highlighting the efficacy of the Hierarchical Global-Local Downsample algorithm in preserving essential data attributes. As

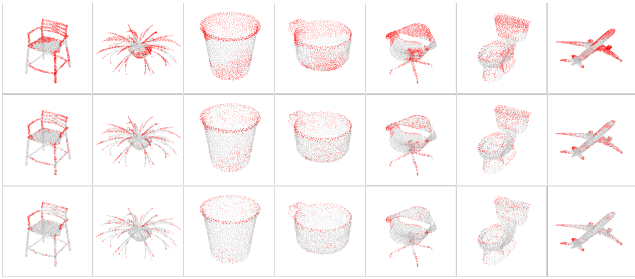


Fig. 4 Hierarchical deep downsampling. The visual representation from top to bottom depicts the evolution of point cloud information following three stages of downsampling. The elements depicted in red symbolize the point cloud post-sampling.

we traverse from left to right, we observe the varying feature information expressed by different objects, underlining the capacity of this methodology to capture and illustrate a wide array of object-specific characteristics in an efficient and concise manner.

3.4 Transformer Attention.

The algorithm 3 begins with the definition of the Transformer Decoder, which calculates the self-attention of the input, computes multi-head attention of the self-attention and memory, and applies a feed-forward neural network. After that, the Transformer Decoder is applied within the Transformer Attention. The input is rearranged, transformed through the decoder, rearranged again, and then normalized twice before returning the output.

Algorithm 3 Transformer Attention

Require: Input tensor $x \in \mathbb{R}^{B \times C \times N}$

Ensure: Output tensor $y \in \mathbb{R}^{B \times C \times N}$

Initialize Transformer Decoder with the necessary parameters

▷ Step 1: Apply Transformer Decoder on rearranged input
Rearrange x to have dimensions 'N B C'

Apply Transformer Decoder on rearranged x to get the transformed tensor

Rearrange the transformed tensor back to 'B C N'

▷ Step 2: Normalization and Finalization

(BN1) on the rearranged tensor

(BN2) on the output of the previous step

return Result from BN2

3.5 Loss function.

In the field of 3D point cloud analysis, the CrossEntropyLoss function is frequently used to quantify the discrepancy between predicted class probabilities and

the actual labels. This loss function is vital for training models involved in semantic segmentation or classification tasks on 3D point cloud data. For a single point within the point cloud, the CrossEntropyLoss is defined as:

$$L(y, \hat{y}) = - \sum_{c=1}^C y_c \cdot \log(\hat{y}_c) \quad (2)$$

Here, $L(y, \hat{y})$ represents the CrossEntropyLoss between the true labels y and the predicted labels \hat{y} . The notation y_c stands for the true label of class c , and \hat{y}_c denotes the predicted probability of class c . The logarithmic term intensifies the penalty for incorrect predictions, aiding the model to enhance its prediction accuracy.

4 Experiments

4.1 Evaluation Metric.

For Classification task, we use Accuracy to present the performance of the methods.

$$Acc = \frac{1}{N} \sum_{i=1}^N 1(y_i = \hat{y}_i) \quad (3)$$

In this equation, N denotes the total number of points, y_i represents the actual class of the i -th point, and \hat{y}_i is the predicted class of the i -th point. The function $1(\cdot)$ is the indicator function, which equals to 1 when $y_i = \hat{y}_i$ (i.e., when the prediction is correct), and 0 otherwise.

In the realm of segmentation tasks, the metrics of Category Mean Intersection over Union (Cat.mIoU) and Instance Mean Intersection over Union (Ins.mIoU) are employed to evaluate the efficacy of our proposed methods.

Cat.mIoU is utilized to assess the performance of semantic segmentation models. It quantifies the intersection-over-union (IoU) for each category or class and computes the average over all categories. The Cat.mIoU is mathematically represented as:

$$Cat.mIoU = \frac{1}{C} \sum_{i=1}^C \frac{TP_i}{TP_i + FP_i + FN_i} \quad (4)$$

In this equation, C denotes the total number of categories or classes. TP_i , FP_i , and FN_i represent the count of true positives, false positives, and false negatives for the category i , respectively.

IMIoU, on the other hand, is a metric employed for instance segmentation tasks. It measures the

intersection-over-union (IoU) between predicted and ground truth instances, and calculates the mean across all instances. The Ins.mIoU is mathematically depicted as:

$$Ins.mIoU = \frac{1}{N} \sum_{j=1}^N \frac{TP_j}{TP_j + FP_j + FN_j} \quad (5)$$

Here, N corresponds to the total number of instances. TP_j , FP_j , and FN_j signify the count of true positives, false positives, and false negatives for instance j , respectively. These metrics provide an encompassing overview of the model’s performance across different aspects of the segmentation task.

4.2 Data and setting

To validate our method, we carry out a series of experiments using ModelNet40 and ShapeNet datasets. During the training phase, we employed the AdamW optimizer with an initial learning rate of 1×10^{-4} and utilized a cosine annealing schedule to gradually decay the learning rate to 1×10^{-8} over the course of 400 epochs, while maintaining a batch size of 16. Additionally, we incorporated a weight decay hyperparameter of 1×10^{-5} to regulate the network weights, and introduced dropout with a probability of 0.5 in the last two fully connected layers. These specific choices of hyperparameters and regularization techniques were carefully selected to optimize the training process, ensure model convergence, and enhance the overall performance and generalization capability of the network.

4.3 Results

quantitative analysis. A thorough quantitative analysis was conducted to evaluate the performance of our proposed methodology in both classification and segmentation tasks, utilizing the ModelNet40 and ShapeNet Part datasets respectively in Table 1 and Table 2. Despite operating with a reduced number of sample points, our method consistently exhibited superior performance, as substantiated by the empirical results. In essence, our approach demonstrated an exceptional capability to succinctly capture the intricate patterns inherent in the sampled point cloud outlines. This attests to its effectiveness as a tool for point cloud analysis, further emphasizing the significance of our contribution to the field.

Table 1 Classification performance on ModelNet40.

Method	Overall Accuracy
PointNet [13]	89.2 %
PointNet++ [14]	91.9 %
[18]	92.4 %
DGCNN [17]	92.9 %
PointCNN [30]	92.2 %
PointConv [31]	92.5 %
PVCNN [32]	92.4 %
KPConv [11]	92.9 %
PointASNL [15]	93.2 %
PT ¹ [19]	92.8 %
PT ² [33]	93.7 %
PRA-Net [34]	93.7 %
PAConv [35]	93.6 %
CurveNet [16]	93.8 %
DeltaConv [36]	93.8 %
HEA-Net	93.8

Table 2 Segmentation results on ShapeNet Part.

Method	Cat. mIoU	Ins. mIoU
PointNet [13]	80.4%	83.7%
PointNet++ [14]	81.9%	85.1%
SpiderCNN [18]	82.4%	85.3%
DGCNN [17]	82.3%	85.2%
SPLATNet [37]	83.7%	85.4%
PointCNN [30]	84.6%	86.1%
PointConv [31]	82.8%	85.7%
KPConv [11]	85.0%	86.2%
PT ¹ [19]	-	85.9%
PT ² [33]	83.7%	86.6%
PRA-Net [34]	83.7%	86.3%
PAConv [35]	84.6%	86.1%
CurveNet [16]	-	86.6%
StratifiedTransformer [38]	85.1%	86.6%
HEA-Net	83.9%	85.9%

Qualitative analysis. Complementary to our quantitative findings in In Figure 5 and Figure 6, we showcase a set of qualitative results, as illustrated in the accompanying figure. Through this visual representation, we aim to provide a comprehensive depiction of the performance characteristics of our proposed methodology. These results serve as valuable evidence to substantiate the efficacy of our approach in practical scenarios, offering a tangible and intuitive understanding of its capabilities. By presenting these qualitative findings, we enhance the comprehensibility and transparency of our research, enabling readers to gain deeper insights into the practical implications and potential applications of our proposed methodology.

4.4 Ablation Study

In order to conduct a rigorous comparative analysis, our proposed sampling technique is systematically evaluated alongside established methodologies, includ-

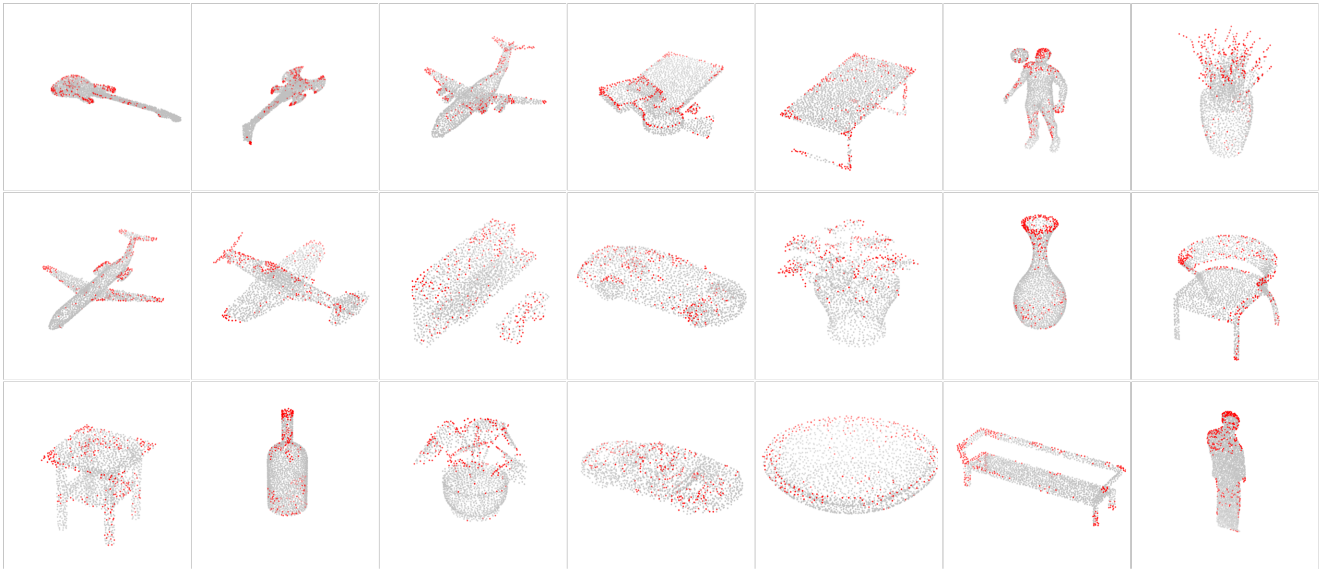


Fig. 5 Visualization of varied shape sampling results are generated by HEA-Net with all shapes being drawn from the test set.

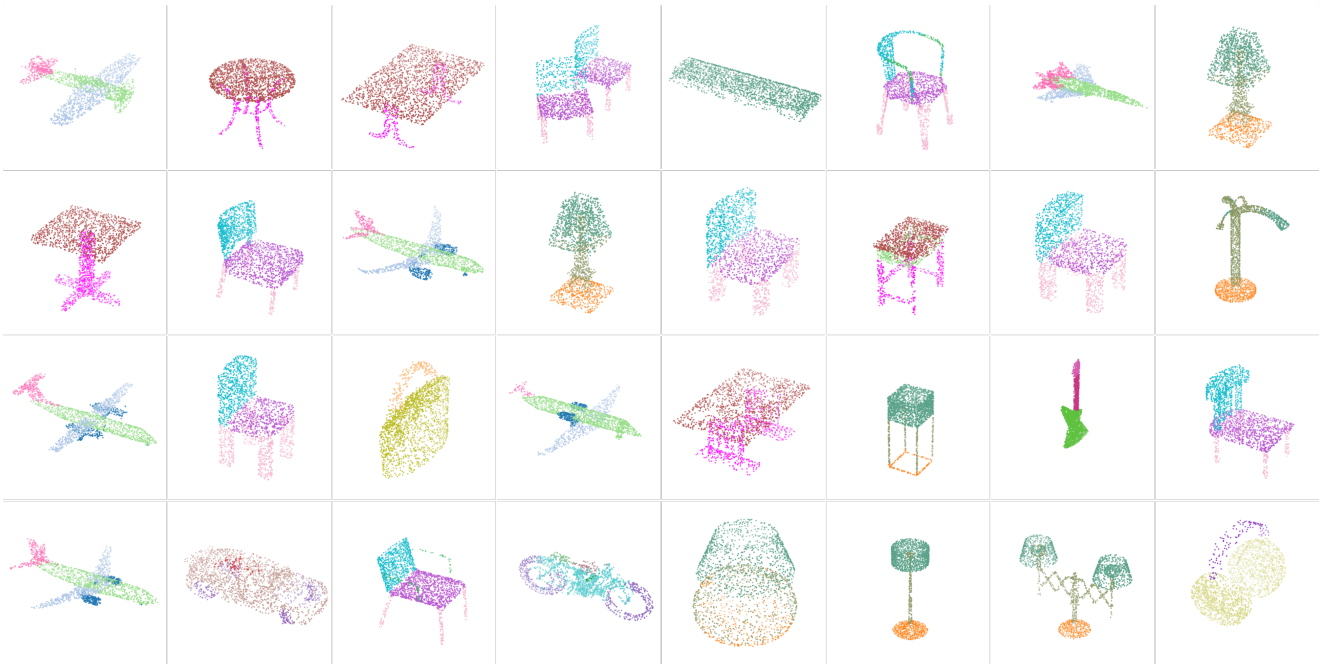


Fig. 6 We provide a visualization of segmentation results as the point clouds of different shapes undergo downsampling. All shapes are from test set.

ing Random Sampling (RS), Farthest Point Sampling (FPS), and recent learning-based approaches such as S-Net, SampleNet, and LightTN. This evaluation follows a standardized evaluation framework employed in prior research studies, as visually illustrated in Figure 8. The primary objective of this study is to assess the classification performance on the ModelNet40 dataset, utilizing the PointNet architecture as the baseline network. By systematically evaluating various sampling approaches across multiple sampling sizes, a comprehensive assess-

ment of their relative performance and efficacy is conducted, contributing to the advancement of the field and providing valuable insights for future research endeavors.

5 Discussion

In our current research focus on indoor object analysis, we have applied our edge-aware learning method.

However, extending this approach to outdoor objects presents unique challenges due to the complex and diverse nature of outdoor scenes. Outdoor environments encompass a wide range of factors, including varying lighting conditions, occlusions from natural elements, and intricate background structures, which complicate edge analysis. Effectively capturing hierarchical edge information becomes crucial for accurate outdoor object analysis. Nonetheless, addressing these challenges and extending edge-aware learning to outdoor contexts offers promising opportunities to enhance computer vision systems in real-world applications such as autonomous driving, surveillance, and environmental monitoring.

Additionally, striking a balance between achieving high accuracy and managing computational complexity is a key consideration. Future work involves expanding the applicability of our method to a broader range of applications, including outdoor scenarios, and exploring potential enhancements to our proposed framework. This entails investigating novel strategies to address the unique characteristics and challenges of outdoor scenes, as well as optimizing the trade-off between accuracy and computational efficiency. Such advancements will contribute to the advancement of edge-aware learning techniques and their broader adoption in diverse real-world scenarios.

Table 3 Our method is assessed against other prevalent sampling techniques, utilizing diverse sampling sizes within the ModelNet40 classification benchmark for a comprehensive comparison.

Method	$M = 512$	$M = 256$	$M = 128$
Voxel	73.82	73.50	68.15
RS	87.52	77.09	56.44
FPS [4]	88.34	83.64	70.34
S-NET [5]	87.80	82.38	77.53
PST-NET [23]	87.94	83.15	80.11
SampleNet [6]	88.16	84.27	80.75
MOPS-Net [39]	86.67	86.63	86.06
DA-Net [7]	89.01	86.24	85.67
LighTN [24]	89.91	88.21	86.26
APES [29]	90.81	90.40	89.77
HEA-Net	93.75	92.26	90.24

6 Conclusion

The human visual system relies extensively on edge and part information for object recognition, serving as inspiration for edge-awareness in computer vision. In this paper, we propose a novel framework for learning from 3D point cloud data, specifically addressing object classification and segmentation tasks. Our approach inte-

grates the strengths of both local and global network learning paradigms, complemented by edge-focused local and global embeddings that enhance the model’s interpretive capacities. Furthermore, we leverage a hierarchical, transformer-based architecture to improve the efficiency of point cloud processing and enable deeper structural comprehension. Through extensive experiments, we validate the efficacy of our proposed framework, demonstrating superior performance in object classification and segmentation compared to state-of-the-art methods. Our work paves the way for further exploration of edge-awareness in 3D point cloud analysis, advancing the frontiers of computer vision research.

References

1. Zhirong Wu, Shuran Song, Aditya Khosla, Fisher Yu, Linguang Zhang, Xiaoou Tang, and Jianxiong Xiao. 3d shapenets: A deep representation for volumetric shapes. In *Proceedings of the IEEE conference on computer vision and pattern recognition*, pages 1912–1920, 2015.
2. Angel X Chang, Thomas Funkhouser, Leonidas Guibas, Pat Hanrahan, Qixing Huang, Zimo Li, Silvio Savarese, Manolis Savva, Shuran Song, Hao Su, et al. Shapenet: An information-rich 3d model repository. *arXiv preprint arXiv:1512.03012*, 2015.
3. Angela Dai, Angel X Chang, Manolis Savva, Maciej Halber, Thomas Funkhouser, and Matthias Nießner. Scannet: Richly-annotated 3d reconstructions of indoor scenes. In *Proceedings of the IEEE conference on computer vision and pattern recognition*, pages 5828–5839, 2017.
4. Yuval Eldar, Michael Lindenbaum, Moshe Porat, and Yehoshua Y Zeevi. The farthest point strategy for progressive image sampling. *IEEE Transactions on Image Processing*, 6(9):1305–1315, 1997.
5. Oren Dovrat, Itai Lang, and Shai Avidan. Learning to sample. In *Proceedings of the IEEE/CVF Conference on Computer Vision and Pattern Recognition*, pages 2760–2769, 2019.
6. Itai Lang, Asaf Manor, and Shai Avidan. Samplenet: Differentiable point cloud sampling. In *Proceedings of the IEEE/CVF Conference on Computer Vision and Pattern Recognition*, pages 7578–7588, 2020.
7. Yanan Lin, Yan Huang, Shihao Zhou, Mengxi Jiang, Tianlong Wang, and Yunqi Lei. Da-net: Density-adaptive downsampling network for point cloud classification via end-to-end learning. In *2021 4th International Conference on Pattern Recognition and Artificial Intelligence (PRAI)*, pages 13–18. IEEE, 2021.

8. Yicheng Zhang, Lei Li, Li Song, Rong Xie, and Wenjun Zhang. Fact: fused attention for clothing transfer with generative adversarial networks. In *Proceedings of the AAAI Conference on Artificial Intelligence*, volume 34, pages 12894–12901, 2020.
9. Meng Wu, Lei Li, and Hongyan Li. Fase: Feature-based similarity search on ecg data. In *2019 IEEE International Conference on Big Knowledge (ICBK)*, pages 273–280. IEEE, 2019.
10. Lei Li, Tianfang Zhang, Stefan Oehmcke, Fabian Gieseke, and Christian Igel. Mask-fpan: Semi-supervised face parsing in the wild with de-occlusion and uv gan. *arXiv preprint arXiv:2212.09098*, 2022.
11. Hugues Thomas, Charles R Qi, Jean-Emmanuel Deschaud, Beatriz Marcotegui, François Goulette, and Leonidas J Guibas. Kpconv: Flexible and deformable convolution for point clouds. In *Proceedings of the IEEE/CVF international conference on computer vision*, pages 6411–6420, 2019.
12. Tianfang Zhang, Lei Li, Siying Cao, Tian Pu, and Zhenming Peng. Attention-guided pyramid context networks for detecting infrared small target under complex background. *IEEE Transactions on Aerospace and Electronic Systems*, 2023.
13. Charles R Qi, Hao Su, Kaichun Mo, and Leonidas J Guibas. Pointnet: Deep learning on point sets for 3d classification and segmentation. In *Proceedings of the IEEE conference on computer vision and pattern recognition*, pages 652–660, 2017.
14. Charles Ruizhongtai Qi, Li Yi, Hao Su, and Leonidas J Guibas. Pointnet++: Deep hierarchical feature learning on point sets in a metric space. *Advances in neural information processing systems*, 30, 2017.
15. Xu Yan, Chaoda Zheng, Zhen Li, Sheng Wang, and Shuguang Cui. Pointasnl: Robust point clouds processing using nonlocal neural networks with adaptive sampling. In *Proceedings of the IEEE/CVF conference on computer vision and pattern recognition*, pages 5589–5598, 2020.
16. AAM Muzahid, Wangen Wan, Ferdous Sohel, Lianyao Wu, and Li Hou. Curvenet: Curvature-based multitask learning deep networks for 3d object recognition. *IEEE/CAA Journal of Automatica Sinica*, 8(6):1177–1187, 2020.
17. Yue Wang, Yongbin Sun, Ziwei Liu, Sanjay E Sarma, Michael M Bronstein, and Justin M Solomon. Dynamic graph cnn for learning on point clouds. *Acm Transactions On Graphics (tog)*, 38(5):1–12, 2019.
18. Yifan Xu, Tianqi Fan, Mingye Xu, Long Zeng, and Yu Qiao. Spidernn: Deep learning on point sets with parameterized convolutional filters. In *Proceedings of the European conference on computer vision (ECCV)*, pages 87–102, 2018.
19. Nico Engel, Vasileios Belagiannis, and Klaus Dietmayer. Point transformer. *IEEE Access*, 9:134826–134840, 2021.
20. Stefan Oehmcke, Lei Li, Jaime Revenga, Thomas Nord-Larsen, Katerina Trepekli, Fabian Gieseke, and Christian Igel. Deep learning based 3D point cloud regression for estimating forest biomass. In *International Conference on Advances in Geographic Information Systems (SIGSPATIAL)*. ACM, 2022.
21. Jaime C Revenga, Katerina Trepekli, Stefan Oehmcke, Rasmus Jensen, Lei Li, Christian Igel, Fabian Cristian Gieseke, and Thomas Friborg. Above-ground biomass prediction for croplands at a sub-meter resolution using uav-lidar and machine learning methods. *Remote Sensing*, 14(16):3912, 2022.
22. Stefan Oehmcke, Lei Li, Jaime C Revenga, Thomas Nord-Larsen, Katerina Trepekli, Fabian Gieseke, and Christian Igel. Deep learning based 3d point cloud regression for estimating forest biomass. In *Proceedings of the 30th International Conference on Advances in Geographic Information Systems*, pages 1–4, 2022.
23. Xu Wang, Yi Jin, Yigang Cen, Congyan Lang, and Yidong Li. Pst-net: point cloud sampling via point-based transformer. In *Image and Graphics: 11th International Conference, ICIG 2021, Haikou, China, August 6–8, 2021, Proceedings, Part III 11*, pages 57–69. Springer, 2021.
24. Xu Wang, Yi Jin, Yigang Cen, Tao Wang, Bowen Tang, and Yidong Li. Lightn: Light-weight transformer network for performance-overhead trade-off in point cloud downsampling. *arXiv preprint arXiv:2202.06263*, 2022.
25. Tianfang Zhang, Lei Li, Christian Igel, Stefan Oehmcke, Fabian Gieseke, and Zhenming Peng. Lr-csnet: Low-rank deep unfolding network for image compressive sensing. *arXiv preprint arXiv:2212.09088*, 2022.
26. Tianfang Zhang, Lei Li, Siying Cao, Tian Pu, and Zhenming Peng. Attention-guided pyramid context networks for detecting infrared small target under complex background. *IEEE Transactions on Aerospace and Electronic Systems*, pages 1–13, 2023. doi: 10.1109/TAES.2023.3238703.
27. Changsheng Zhou, Chao Yuan, Hongxin Wang, Lei Li, Stefan Oehmcke, Junmin Liu, and Jigen Peng. Multi-scale pseudo labeling for unsupervised deep edge detection. *Available at SSRN 4425635*.

28. Lei Li, Tianfang Zhang, Stefan Oehmcke, Fabian Gieseke, and Christian Igel. Buildseg buildseg: A general framework for the segmentation of buildings. *Nordic Machine Intelligence*, 2(3), 2022.
29. Chengzhi Wu, Junwei Zheng, Julius Pfommer, and Jürgen Beyerer. Attention-based point cloud edge sampling. In *Proceedings of the IEEE/CVF Conference on Computer Vision and Pattern Recognition*, pages 5333–5343, 2023.
30. Yangyan Li, Rui Bu, Mingchao Sun, Wei Wu, Xinhan Di, and Baoquan Chen. Pointcnn: Convolution on x-transformed points. *Advances in neural information processing systems*, 31, 2018.
31. Wenxuan Wu, Zhongang Qi, and Li Fuxin. Pointconv: Deep convolutional networks on 3d point clouds. In *Proceedings of the IEEE/CVF Conference on computer vision and pattern recognition*, pages 9621–9630, 2019.
32. Zhijian Liu, Haotian Tang, Yujun Lin, and Song Han. Point-voxel cnn for efficient 3d deep learning. *Advances in Neural Information Processing Systems*, 32, 2019.
33. Hengshuang Zhao, Li Jiang, Jiaya Jia, Philip HS Torr, and Vladlen Koltun. Point transformer. In *Proceedings of the IEEE/CVF international conference on computer vision*, pages 16259–16268, 2021.
34. Silin Cheng, Xiwu Chen, Xinwei He, Zhe Liu, and Xiang Bai. Pra-net: Point relation-aware network for 3d point cloud analysis. *IEEE Transactions on Image Processing*, 30:4436–4448, 2021.
35. Mutian Xu, Runyu Ding, Hengshuang Zhao, and Xiaojuan Qi. Paconv: Position adaptive convolution with dynamic kernel assembling on point clouds. In *Proceedings of the IEEE/CVF Conference on Computer Vision and Pattern Recognition*, pages 3173–3182, 2021.
36. Ruben Wiersma, Ahmad Nasikun, Elmar Eise mann, and Klaus Hildebrandt. Deltaconv: Anisotropic point cloud learning with exterior calculus. *arXiv preprint arXiv:2111.08799*, 2021.
37. Hang Su, Varun Jampani, Deqing Sun, Subhransu Maji, Evangelos Kalogerakis, Ming-Hsuan Yang, and Jan Kautz. Splatnet: Sparse lattice networks for point cloud processing. In *Proceedings of the IEEE conference on computer vision and pattern recognition*, pages 2530–2539, 2018.
38. Xin Lai, Jianhui Liu, Li Jiang, Liwei Wang, Hengshuang Zhao, Shu Liu, Xiaojuan Qi, and Jiaya Jia. Stratified transformer for 3d point cloud segmentation. In *Proceedings of the IEEE/CVF Conference on Computer Vision and Pattern Recognition*, pages 8500–8509, 2022.
39. Yue Qian, Junhui Hou, Qijian Zhang, Yiming Zeng, Sam Kwong, and Ying He. Mops-net: A matrix optimization-driven network for task-oriented 3d point cloud downsampling. *arXiv preprint arXiv:2005.00383*, 2020.